DOI: 10.1002/anie.201203201

Energy Storage

Nanostructured Electrodes for High-Performance Pseudocapacitors

*Qi Lu, Jingguang G. Chen, and John Q Xiao**

electrodes · metal oxides · nanomaterials · pseudocapacitors · supercapacitors

The depletion of traditional energy resources as well as the desire to reduce high CO_2 emissions associated with energy production means that energy storage is now becoming more important than ever. New functional electrode materials are urgently needed for next-generation energy storage systems, such as supercapacitors or batteries, to meet the ever increasing demand for higher energy and power densities. Advances in nanotechnology are essential to meet those future challenges. It is critical to develop ways of synthesizing new nanomaterials with enhanced properties or combinations of properties to meet future challenges. In this Minireview we discuss several important recent studies in developing nanostructured pseudocapacitor electrodes, and summarize three major parameters that are the most important in determining the performance of electrode materials. A technique to optimize these parameters simultaneously and to achieve both high energy and power densities is also introduced.

1. Introduction

The storage of electricity will become more and more important in future societies.[1] Whether to buffer the power grids of wind/solar power plants for their intermittent availabilities or to boost the myriad applications from portable consumer electronic devices to electrical vehicles, the desire for advanced high-performance energy storage devices will be extremely high. Nanotechnologies will play a critical role in advancing the development to store energy.

Supercapacitors are highly desirable energy storage devices because of their ability to simultaneously deliver high power and reasonably high energy densities. Unfortunately, several major problems have prevented supercapacitors from becoming commercially viable primary power supplies. In particular, the energy density is not high enough, and most fabrication processes are not appropriate for manufacture at large scales.

Supercapacitors either store energy between the electrode and electrolyte interfaces as electrochemical double-layer capacitors (EDLCs), or further employ a fast and reversible redox reaction between electrodes and the electroactive species in electrolytes as pseudocapacitors.[2] Because such redox reactions usually take place in metal oxides where metal ions have multiple valence states, materials such as NiO, MnO_2, and RuO_2 are the most investigated candidates because of their potential to combine the advantages from both mechanisms.[3]

Progress in pseudocapacitor technology has benefited greatly by moving from conventional to nanostructured electrodes.[4] The large surface area created by nanoscale structures significantly enhances the efficiency in utilizing the electrode material and therefore improves the electrode performance. However, the application of nanostructured materials certainly does not automatically lead to enhancement. For example, high surface area nanoporous electrodes usually exhibit ill-defined pore structures and a wide pore size distribution, which inhibits the diffusion of electrolyte ions at fast charge/discharge rates and therefore affects the material

[*] Dr. Q. Lu
Department of Chemical and Biomolecular Engineering
University of Delaware, Newark, DE 19716 (USA)
Prof. Dr. J. G. Chen
Department of Chemical Engineering
Columbia University, New York, NY 10027 (USA)
Prof.Dr. J. Q. Xiao
Department of Physics and Astronomy
University of Delaware, Newark, DE 19716 (USA)
E-mail: jqx@udel.edu

utilization. To enhance the utilization of electrode material for achieving maximum performance, it is vital to design electrode structures with large surface areas for efficient access of electrolyte ions. With the purpose of establishing a scientific basis for the design of high-performance nanostructured electrodes, this minireview summarizes three key parameters that are believed to be most important in determining electrode performance. Their contributions to the performance improvement are illustrated by several important recent studies.

2. Important Parameters for High Performance

2.1. Electrode Structure

While pseudocapacitor electrodes with large surface areas can be achieved by making materials at the nanoscale, it is difficult to directly investigate the transport of electrolyte ions inside the electrode nanostructures. The ion diffusion process is always entangled with complicated redox reactions. However, the driving force of the diffusion process is primarily related to the difference in chemical potential caused by the concentration gradient, which is the same as in nanostructured EDLC-type electrodes. For this reason, several insightful EDLC papers were also included for discussion in this section because they provide clear guidance for the structural design of pseudocapacitor electrodes.

Numerous efforts have been focused on developing techniques for fabricating nanostructured materials.[5] Despite significant progress, however, various negative impacts come along with untailored structures. For example, in carbon-based electrodes in which the pore structures are usually mesoporous (2–50 nm), the specific capacitance (SC) normalized to specific surface area (SSA) drops as the pore size decreases (Figure 1, zone III and zone IV).[1d] Therefore the enhanced surface area becomes less efficient in contributing to the total charge storage as shown in the inset of Figure 1.[6] Huang et al. explained this phenomenon theoretically by assuming that the mesopores are cylindrical, so that the specific capacitance with respect to SSA could be written in the form of Equation (1),[7] where b is the pore radius and d is the distance between approaching electrolyte ion and the carbon surface.

$$C/A = \frac{\varepsilon_r \varepsilon_0}{b \ln\left(\frac{b}{b-d}\right)} \quad (1)$$

The theoretical fitting is shown as lines in Figure 1, which accounts for the experimental data exceptionally well. In the micropore region, an anomalous increase of specific capacitance was observed (Figure 1, zone I) owing to the loss of the solvation shell, making the distance between the electrolyte ions and the electrode surface closer.[8] The phenomenon can be described by Equation (2),[7] where a_0 is the radius of the electrolyte ion (desolvated).

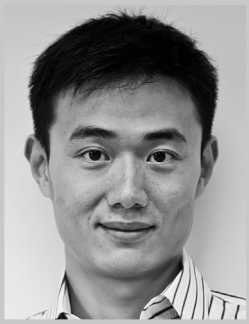

Dr. Qi Lu studied material science and engineering at Zhejiang University and completed his Ph.D. in physics at University of Delaware with Prof. Dr. Xiao. He is currently a postdoctoral researcher in the Department of Chemical and Biomolecular Engineering at University of Delaware. His current research is focused on the development of lithium-ion batteries and supercapacitors for high-performance energy storage.

Dr. Jingguang Chen is the Thayer Lindsley Professor of Chemical Engineering at Columbia University. He started his career at the Exxon Corporate Research Laboratories before joining the faculty at the University of Delaware. His current research activities include experimental and theoretical studies aimed at the utilization of materials for catalytic and electrochemical applications.

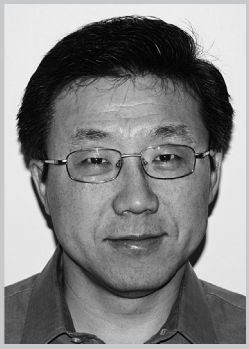

Dr. John Xiao is the Unidel Professor of Physics and Astronomy, the director of the Center for Spintronics and Biodetection at University of Delaware, and a fellow of American Physical Society. His research interests include the studies of novel nanostructured materials for spintronics, microwave, and electrochemical applications.

$$C/A = \frac{\varepsilon_r \varepsilon_0}{b \ln\left(\frac{b}{a_0}\right)} \quad (2)$$

One of the important questions is whether the high capacitance contributed from micropores would still be retained for high power applications, as the diffusion depth λ of electrolyte ions in a cylindrical nanopore at fast charge/discharge rate is significantly reduced in finite pore sizes according to Equation (3),[9] where r is the pore radius, κ is the electrolyte conductivity, C_d is the electric double-layer capacitance, and ω is the angular frequency of charge/discharge. The reduced ion penetrability (λ/l_p, where l_p is the pore length) could be a possible reason why it is commonly found that the specific capacitances of nanostructured electrodes always decrease as the charge/discharge rates increase.

$$\lambda = \frac{1}{2}\sqrt{\frac{\kappa r}{C_d \omega}} \quad (3)$$

The effect of the pore length and diffusion depth on the electrode performances was examined by Xia et.al.[10] The authors synthesized highly ordered mesoporous carbon with both short pore lengths (SOMC) of 200–300 nm and long pore

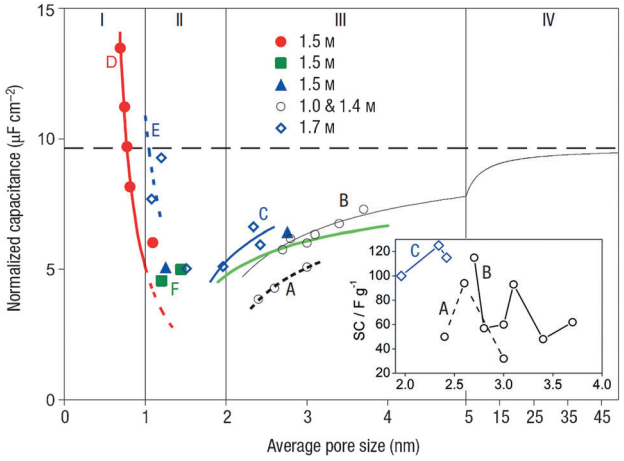

Figure 1. Specific capacitance normalized by SSA as a function of pore size for different carbon samples. All samples were tested in the same electrolyte (NEt_4^+, BF_4^- in acetonitrile) with several different concentrations. Line fittings in the mesoporous and microprous regimes are obtained using Equation (1) and Equation (2) separately. Various carbon materials, including templated microporous carbon (A and B), activated mesoporous carbon (C), microporous carbide-derived carbon (D and F), and microporous activated carbon (E), are presented. Inset: Specific capacitance normalized by electrode mass as a function of mesopore size. Reproduced from reference [1d].

lengths (LOMC) of up to tens of micrometers as electrode materials using hard silica templates. Except for the pore length, these two types of electrodes exhibited almost identical pore size distribution and surface area. The specific capacitance (SSA) of SOMC electrodes exhibited a 40% higher value than that of LOMC electrodes, indicating the significant inhibition of material utilization caused by the reduction of ion penetrability. Using electrochemical impedance measurements, the LOMC electrodes also showed a 25% higher resistance of charge in electrode pores than SOMC electrodes, suggesting that pores with longer lengths are more difficult to access. These studies clearly pointed out that one of the important keys for high-performance electrodes is not simply the use of nanomaterials with high surface area, but a tailored electrode structure with high ion accessibility even at a fast charge/discharge rate.

In addition to pore geometries, the alignment of nanopores is another important factor because the diffusion of electrolyte ions only favors the pores in parallel with electrical driving forces:[11] Hata and co-workers prepared aligned and densely packed single-walled carbon nanotube (SWNTs) electrodes with a well-defined pore structure either parallel or perpendicular to the electrical field between the current collectors (Figure 2). A larger diffusion coefficient of $1\times10^{-5}\,cm^2s^{-1}$ was found in the parallel direction electrode, which was close to the theoretical limit value of $2.6\times10^{-5}\,cm^2s^{-1}$, and is significantly larger than that in the perpendicular counterpart ($8\times10^{-7}\,cm^2s^{-1}$). The specific capacitance showed no obvious differences at a sufficiently low charge/discharge rate. However, as the charge/discharge rate was increased by an order in magnitude, a more than 60% specific capacitance loss was observed in the supercapacitor with a perpendicular electrode, while the decrease

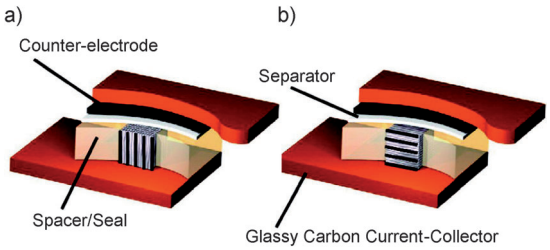

Figure 2. Impact of SWNT orientation on capacitance performance. a) Cross-sectional view of the device with the solid-cube electrode in the parallel orientation. b) Cross-sectional view of the device with the solid-cube electrode in the perpendicular orientation. Reproduced from reference [11].

was only about 10% in a parallel electrode, indicating that it is essential to align the electrode pores in the dominant diffusion direction for high power applications.

The influence of the degree of electrode pore ordering was also explored:[12] A recent theoretical investigation by Gogotsi et al. revealed that in a nanoporous carbon electrode, narrowing down the electrode pore size distribution led to an increase of its stored energy density (Figure 3). This conclusion highlights the importance of a uniform electrode pore structure with an optimized pore size in building high-performance electrodes.

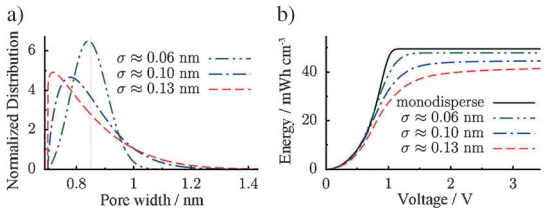

Figure 3. a) Normalized pore size distributions (with identical average pore width of 0.85 nm) used to calculate energy densities. σ is the standard deviation of pore sizes. b) The energy density as a function of voltage for monodisperse porous electrode (average pore width = 0.85 nm; $\sigma = 0$), and for polydisperse porous electrode with the pore size distributions in (a)).

An experimental demonstration can be seen from the work conducted by Xia and Luo, in which porous MnO_2 materials were used as electrodes.[13] As shown in Figure 4c,d, disordered mesoporous MnO_2 ($DMMnO_2$) and ordered mesoporous MnO_2 ($OMMnO_2$) were synthesized as electrode materials using either a self-assembly process or the silica hard template method. The representative cyclic voltammometry curves for these two materials are shown in Figure 4a,b. At low potential scan rates, both types of electrodes exhibited an "ideal" capacitance behavior, that is, the current density weakly depends on the applied potential. However, the cyclic voltammograms of $DMMnO_2$ became seriously distorted as the scan rate increased to above $200\,mV\,s^{-1}$. This phenomenon, which is usually attributed to the high electrode equivalent series resistance (ESR), indicated that $DMMnO_2$ was not suitable for high power operations. It was also observed that in $OMMnO_2$ electrodes, 64% of their initial

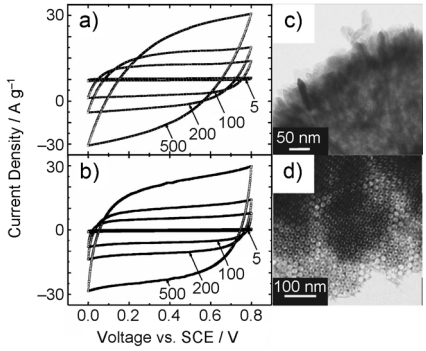

Figure 4. a,b) Cyclic voltammometry curves of a) $DMMnO_2$ and b) $OMMnO_2$ electrodes at various potential scan rates (in $mV s^{-1}$) in 1 M Na_2SO_4 aqueous solution. c,d) TEM images of c) $DMMnO_2$ and d) $OMMnO_2$. Reproduced from reference [13].

capacitance was retained even at a high potential scan rate of $500 mV s^{-1}$, while this number was only 42% in $DMMnO_2$ electrodes even though their pore size was twice as large as that of $OMMnO_2$ electrodes.

Therefore, nanostructured electrodes with enhanced surface area are not a simple panacea for achieving high-performance. Electrodes characterized by the same large surface area may have very different performances. Many nanostructured materials with different structures, such as dendrites, nanorods, or nanotubes, have been studied for pseudocapacitor applications.[14] However, the electrode structures become random and untailored after their typical electrode fabrication process (mixing with polymer binder and conductive additives). However, very little work has yet been done in systematically studying the principles for optimizing electrode architectures, especially those involving redox reactions. In this section, several insightful studies that illustrate how different electrode structures affect the electrode performance are reviewed, from which some qualitative guidelines for the architectural design of nanostructured electrodes with better electrolyte ion accessibility can be obtained.

2.2. Electrode Conductivity

In most of the nanostructured pseudocapacitor electrodes, the loss of medium to high rate capacity is a typical observation. This is because at a high charge/discharge rate, the potential drop across the electrode owing to the resistance to electron conduction is more pronounced. Consequently, the charge/discharge processes can only be localized in a finite volume near the current collector, causing a reduction in electrode material utilization and restricting their high-power applications.[15]

The effect of low conductivity on electrode performances can be studied with various experimental methods. The most straightforward way is to observe a specific capacitance loss at higher potential scanning rates in cyclic voltammometric (CV) measurements or at higher current densities in galvanostatic cycling. A potential drop in galvnostatic cycle curve when switching the current direction is also an indication of non-uniform potential distribution along the electrode, which is usually caused by the electrode resistance.

To overcome the internal electrode resistance, it is highly desirable to either modify the electrode materials for better conductivity, or to design nanostructured current collectors with increased contact area and enhanced quality of contacts. The former approach was extensively exercised in carbon-based EDLCs. Because of the excellent electrical conductivity of carbon nanotube[16] (single-walled or multi-walled) and graphene[17] owing to the vast electron delocalization within their carbon single layers, these materials were widely studied as EDLC-type electrodes in the hope of replacing traditional active carbon. Although better power performance was achieved with the enhanced electrode conductivity, the fundamentally low specific capacitance of carbon material, and large volume owing to their low material density limited further development.

Metal oxide based pseudocapacitor electrodes, which include both EDLC and Faradic-type charge storage, have much higher theoretical capacitance and volumetric performance. However, they suffer from the intrinsic high resistivity of the electrode materials. The latter approach, which is to develop high efficiency current collectors, therefore becomes crucial to realize the full potential of the electrodes. A recent demonstration of enhanced performance which benefited from such efforts is from the work of Chen et al.[18] As shown in Figure 5a, highly conductive nanoporous gold films were fabricated as current collectors by de-alloying $Au_{35}Ag_{65}$ (atomic ratio) films in HNO_3 solution. Nanocrystalline MnO_2, as the functional electrode material, was then deposited on the surface of the gold network by electroless plating (Figure 5b). The chemically bonded metal/oxide interface (Figure 5c) provides good electrical conductivity. The achieved large specific capacitance (ca. $1145 F g^{-1}$, scaled to the mass of active MnO_2) is close to its theoretical value, indicating the high utilization of electrode materials. More impressively, as the charge/discharge current density was increased by an order of magnitude ($2 A g^{-1}$ to $20 A g^{-1}$) for high-power characterization, the specific capacitances were barely affected (Figure 5e). The simultaneously achieved high charge capacity and power density could only be attributed to the small IR polarization loss owing to high electrode conductivity, resulting in high material utilization even at large charge/discharge current densities.

An alternative approach worth noting here is the work by Lee and Liu.[19] Instead of developing a highly conductive current collector as support for the functional material, the authors coated the functional material with a conductive and porous layer, which was believed to enhance electron transport and ion diffusion. As shown in Figure 6a–d, coaxial MnO_2 and poly(3,4-ethylenedioxythiophene) (PEDOT) nanowire arrays were synthesized by a one-step co-electrodepostion method using commercial anodic aluminum oxide (AAO) templates. The thickness of the conductive PEDOT shell could be varied by tuning the deposition potential, while the diameter (ca. 200 nm) of the composite wire was fixed by the template. At small charge/discharge current densities ($5 mA cm^{-2}$), the specific capacitance of coaxial wire arrays did not exhibit obvious differences than that of pure MnO_2

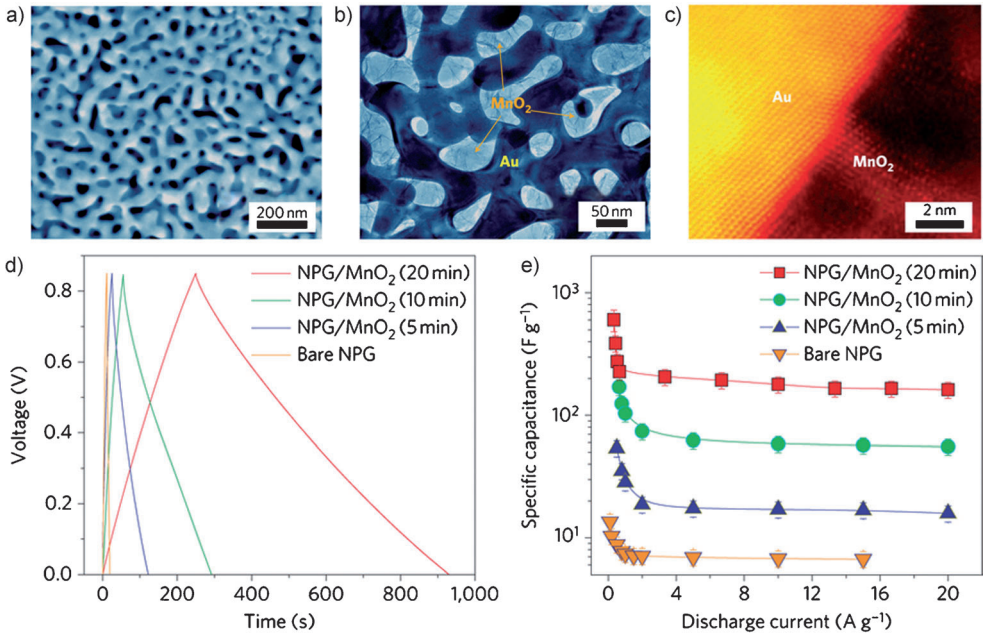

Figure 5. a) SEM image of as de-alloyed nanoporous gold films with a characteristic length of about 40 nm. b) Bright-field TEM image of the nanoporous gold/MnO_2 hybrid with a MnO_2 plating time of 20 min. c) High-angle annular dark-field STEM image taken from a gold/MnO_2 interface region. Nanocrystalline MnO_2 epitaxially grows on the gold surface, forming a chemically bonded metal/oxide interface. d) Cyclic chronopotentiometric curves with a charge/discharge current density of 0.5 $A g^{-1}$ and e) Specific capacitances (scaled to the total electrode mass including the porous gold substrate) derived from the discharge portion of cyclic chronopotentiometry versus discharge current densities for electrodes prepared on MnO_2 at various plating times. Reproduced from reference [18].

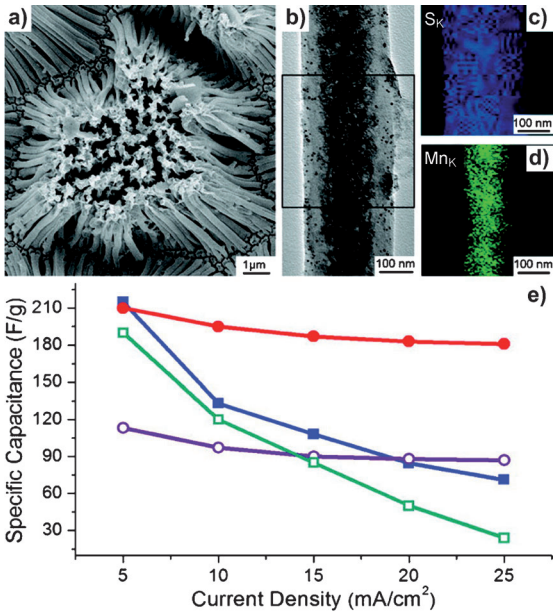

Figure 6. a) SEM image of MnO_2/PEDOT coaxial nanowire arrays. b) TEM image from a single coaxial nanowire. c,d) EDS maps of c) S and d) Mn from the boxed area in (b). Scale bars: 1 μm (a), 100 nm (b–d). e) Specific capacitance (scaled to the mass of MnO_2) of MnO_2 nanowires (closed blue square), PEDOT nanowires (open purple dots), MnO_2 thin film (open green square), and MnO_2/PEDOT coaxial nanowires (closed red dots) at different charge/discharge current densities. Reproduced from reference [19].

wire arrays or electrochemically deposited MnO_2 films (Figure 6e). However, as the current density was increased to 25 mA cm^{-2}, a more than 60% capacitance loss was observed in electrodes without conductive coating, while this value was much less affected (< 15%) in the coaxial MnO_2/PEDOT nanowire arrays.

The most important advantage of supercapacitors over mediocre batteries is their much higher power densities. However, supercapacitors would lose the meaning of "super" if a higher power density came along with loss of charge capacity. Therefore, for achieving high-performance pseudocapacitor electrodes with both high energy and power densities, the enhancement of electrode conductivity is crucial. A successful illustration can be seen from a recent report from Dai and co-workers.[20] In their work, a two-step process of directly growing $Ni(OH)_2$ nanoplates on highly conductive graphene sheets (GS) was developed (Figure 7a). Intimate contacts between the functional material and current collector were formed by anchoring the $Ni(OH)_2$ onto the GS with both covalent chemical bonding and van der Waals interactions. The thickness of the electrically supported $Ni(OH)_2$ nanoplates is in the range of several nanometers. Therefore, in principle, the IR polarization loss across the $Ni(OH)_2$ plates is negligible even at high charge/discharge current densities of several tens of amperes per material mass. The electrochemical performance (Figure 7d) demonstrated the necessities of such efforts for better electrode conductivity. The high energy density achieved at a high power density (both are scaled to the mass of active $Ni(OH)_2$) is superior to that of controlled electrodes with the same functional

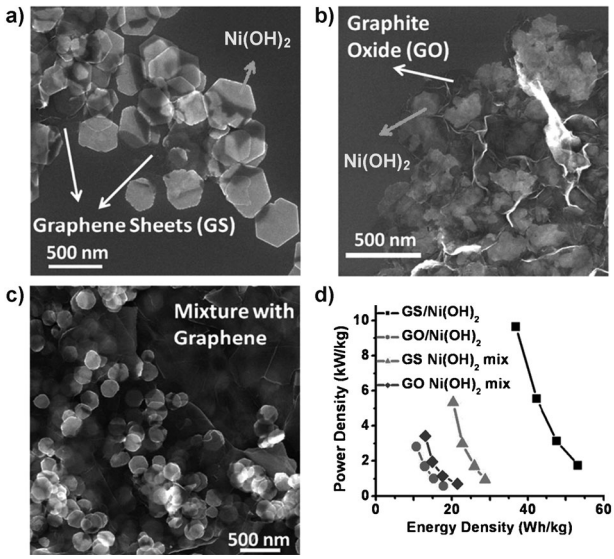

Figure 7. SEM images of a) $Ni(OH)_2$ nanoplates grown on GS, b) $Ni(OH)_2$ nanoparticles grown on graphene oxide (GO), and c) a simple physical mixture of presynthesized free $Ni(OH)_2$ nanoplates and GS. d) Ragone plot (power density versus energy density) of $Ni(OH)_2$ hexagonal nanoplates grown on GS (black), $Ni(OH)_2$ nanoparticles grown on GO (red), and presynthesized $Ni(OH)_2$ hexagonal nanoplates physically mixed with GS (green) and GO (blue). All values were scaled to the mass of active $Ni(OH)_2$ nanoplates. Reproduced from reference [20].

material but with worse electrode conductivity (Figure 7b,c). The usable high power density is among the best results reported to date.

One of the obstacles that inhibit pseudocapacitors based on nanostructured electrodes from becoming commercially feasible is the small mass loading of the functional materials. To retain acceptable electrode conductivity, a large fraction of mass from current collectors (metal foams/grids/plates) and conductive additives is usually employed, which as a result deteriorates the performance of the whole electrode. Therefore, the nanostructured electrodes discussed in this section are useful for proof-of concept studies or for microdevices, but are very unlikely to be used in applications, such as electric vehicles or power grid storage.[21] To merge pseudocapacitors with nanostructured electrodes as primary power suppliers in the future energy storage market, it is crucial to design techniques that are able to deliver the desired electrode conductivity in more efficient manners.

2.3. Electrode Crystallinity

While the EDLC type charge storage is purely a surface phenomenon, the Faradic type charge storage in pseudocapacitor electrodes involves bulk contributions. This conclusion is evident from many studies of a variety of functional materials, such as NiO, MnO_2, and RuO_2,[22] as electrodes with low crystallinity usually exhibit larger specific capacitance than their high crystallinity counterparts. This phenomenon was explained by the fact that the high density of the grain boundaries in structures with fine grains lead to more efficient diffusion channels for electrolyte ions, giving rise to the enhanced utilization of electrode materials.[22e,23]

To obtain more quantitative understandings of the impact of electrode crystallinity on pseudocapacitance performance, a model system based on NiO thin films with well-defined column structures and controlled crystallinity was recently investigated (Figure 8).[23b] The specific capacitances contributed from electrode surfaces and electrode bulk were differentiated by separating the cyclic voltammometric curves into a capacitive portion and a diffusion controlled portion (Figure 9). The plateau region of specific capacitances versus

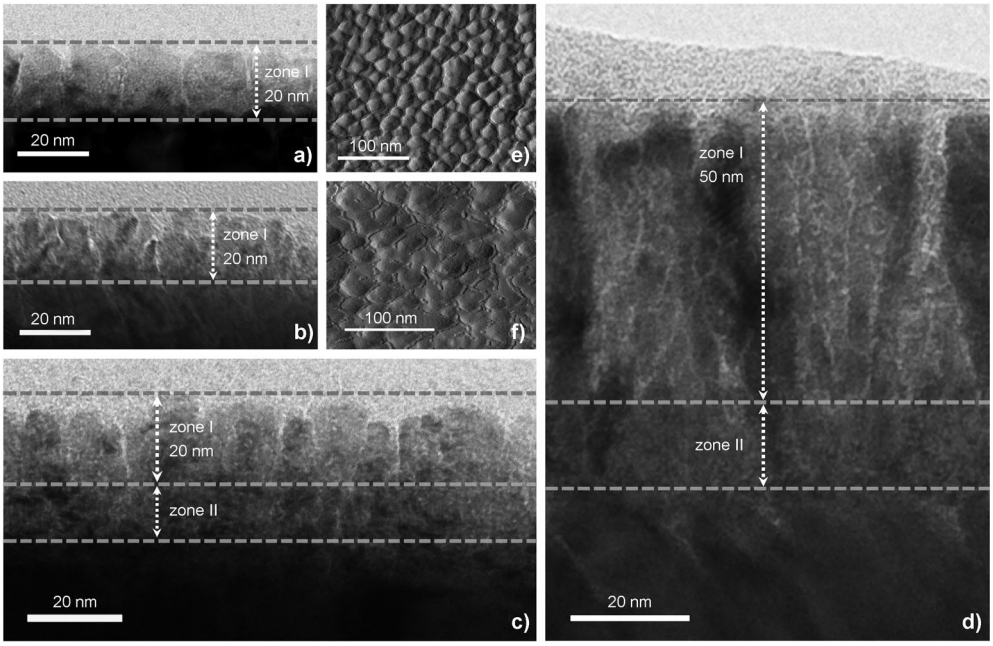

Figure 8. a–d) TEM micrograph at a cross-section of a) 20 nm amorphous NiO thin film, b) 20 nm crystalline NiO thin film, c) 35 nm amorphous NiO film, and d) 70 nm crystalline film. e,f) AFM image at the surface of e) 20 nm amorphous film and f) 40 nm crystalline film.

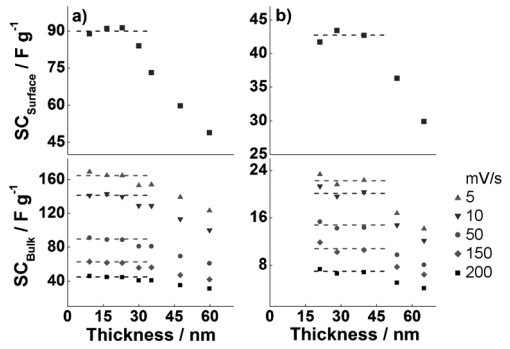

Figure 9. Thickness dependence of specific capacitance contributed from surface (upper panels) and bulk (lower panels) of a) amorphous thin films and b) crystalline thin films.

the film thickness in both amorphous and crystalline electrodes suggests that the electrode material can only be wetted by the electrolyte through column boundaries that cease beyond 20 nm and 50 nm, respectively. The crystalline column diameter (ca. 30 nm) was almost twice as large as that of the amorphous column (ca. 15 nm), leading to the effective surface area per unit volume being twice as large in amorphous films as that in crystalline films inside the plateau region (Figure 8e,f). Consequently, this leads to an important conclusion that the specific capacitance from surface contribution is the same for both amorphous and crystalline films. However, for the same surface area, the specific capacitance from bulk contribution should be at least three times larger in amorphous films than in crystalline films.

Thus although it is a viable approach to increase the accessible electrode surface area for the enhancement of material utilization, it is equally or even more important to tailor the material crystallinity to realize their full potential. Even though the work was conducted on NiO, we believe that the conclusions drawn are also applicable in understanding wide criteria of candidate materials.

3. Electrode Optimization for High Performance

Recent advances in nanotechnologies have greatly advanced the development of high-performance pseudocapacitor electrodes. Despite significant progresses, however, techniques to realize the full potential of electrode material by achieving simultaneously tailored electrode structure, conductivity, and crystallinity are lacking. Moreover, among all the approaches developed to date, the problem of being difficult in industrial scale manufacture still exists. For an attempt to address all these issues, we recently developed a simple and cost-effective process, which is also scalable, for achieving pseudocapacitor electrodes with both high energy and power densities.[23a]

The process starts with the production of nickel nanoparticles by reducing Ni^{2+} ions in high-boiling temperature polyalcohols (Figure 10a). The obtained nanoparticles were mechanically compressed into pellets to form porous prototype electrodes (Figure 10b,c), of which the pore size was optimized by controlling the size of Ni nanoparticles. A very thin platinum coating was deposited onto one side of the pellet which later acts as a current collector. Annealing at different thermal conditions forms a layer of nickel oxide around the porous nickel network which serves as the functional material. The thickness of nickel oxide layer and its crystallite sizes can be tuned for simultaneously achieving high electrode conductivity and small crystallinity. The resulting nanocomposite electrodes are highly porous, mechanically stable, and do not require any further support or additives.

The electrodes prepared at 250 °C exhibited a high conductivity with metallic behavior and very fine nickel oxide particle sizes (Figure 10d,e). The resulting large specific capacitance of 910 F g^{-1} (scaled to the active mass of NiO or ca. 300 F g^{-1} scaled to the total mass of the electrode, including the Ni core network) was not only better than that of their higher temperature counterparts, but also among the

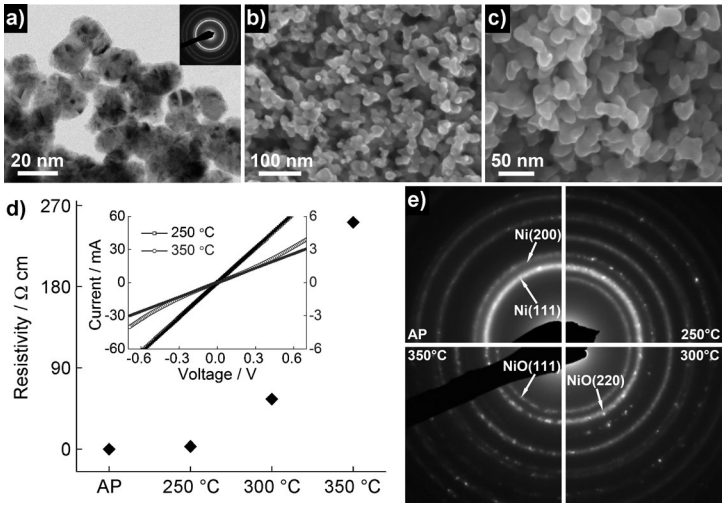

Figure 10. Characterization of the electrode structure: a) TEM image and ED pattern of the as-prepared Ni nanoparticles. SEM images at the b) surface and c) cross-section of the prototype electrode. d,e) Characterization of the conductivity and crystallinity: d) Resistivities of samples prepared at different thermal conditions. Inset: I–V curves and associated linear fits within the range of −0.1 to 0.1 V. At 250 °C the sample behaves like a metal, whereas at 350 °C it shows a tunneling effect because of the isolated conductive metal cores. e) ED patterns of the NiO/Ni nanoparticles oxidized at different temperatures.

best values achieved in the field of pseudocapacitors. By developing a slow charge/fast discharge process (1M KOH aqueous solution was used as electrolyte), a probably state-of-the-art pseudocapacitor performance of both high energy density and high power density was simultaneous achieved.

4. Summary and Outlook

Nanostructured electrodes will undoubtedly boost pseudocapacitors into the next-generation energy storage devices. The goal of this minireview is to provide three important parameters as guidelines in electrode design for achieving high-performance pseudocapacitors: electrode structure, conductivity, and crystallinity. The scientific purpose underneath the guidelines is to enhance the electrode material utilization, especially at fast charge/discharge rates for high-power applications. Future directions of advanced electrode design should include simultaneously tailored electrode structure, conductivity, and crystallinity. The techniques for fabricating those electrodes should facilitate the scalable production for large-scale commercial applications.

The work carried out in the authors' laboratory was supported by the Office Naval Research under the grant of N00014-08-1-0432 and by the US Department of Energy under the grant of DE-FG02-13ER16381. The authors would also like to thank Prof. Karl Unruh and Prof. Feng Jiao for their collaboration and enlightening discussions during the past several years.

Received: April 25, 2012
Revised: July 30, 2012
Published online: January 10, 2013

[1] a) A. S. Aricò, P. Bruce, B. Scrosati, J. M. Tarascon, W. Van Schalkwijk, *Nat. Mater.* **2005**, *4*, 366–377; b) P. G. Bruce, B. Scrosati, J. M. Tarascon, *Angew. Chem.* **2008**, *120*, 2972–2989; *Angew. Chem. Int. Ed.* **2008**, *47*, 2930–2946; c) C. Liu, F. Li, L. P. Ma, H. M. Cheng, *Adv. Mater.* **2010**, *22*, E28; d) P. Simon, Y. Gogotsi, *Nat. Mater.* **2008**, *7*, 845–854.

[2] a) B. E. Conway, *J. Electrochem. Soc.* **1991**, *138*, 1539–1548; b) E. Frackowiak, F. Beguin, *Carbon* **2001**, *39*, 937–950.

[3] a) Z. J. Fan, J. Yan, T. Wei, L. J. Zhi, G. Q. Ning, T. Y. Li, F. Wei, *Adv. Funct. Mater.* **2011**, *21*, 2366–2375; b) J. H. Kim, K. Zhu, Y. F. Yan, C. L. Perkins, A. J. Frank, *Nano Lett.* **2010**, *10*, 4099–4104; c) H. Y. Lee, V. Manivannan, J. B. Goodenough, *C. R. Acad. Sci. Ser. II C* **1999**, *2*, 565–577; d) R. Liu, J. Duay, S. B. Lee, *ACS Nano* **2011**, *5*, 5608–5619; e) K. W. Nam, K. B. Kim, *J. Electrochem. Soc.* **2002**, *149*, A346–A354; f) G. W. Yang, C. L. Xu, H. L. Li, *Chem. Commun.* **2008**, 6537–6539; g) G. L. Cui, L. J. Zhi, A. Thomas, I. Lieberwirth, U. Kolb, K. Mullen, *ChemPhysChem* **2007**, *8*, 1013–1015; h) J. P. Zheng, P. J. Cygan, T. R. Jow, *J. Electrochem. Soc.* **1995**, *142*, 2699–2703; i) W. Sugimoto, H. Iwata, Y. Yasunaga, Y. Murakami, Y. Takasu, *Angew. Chem.* **2003**, *115*, 4226–4230; *Angew. Chem. Int. Ed.* **2003**, *42*, 4092–4096.

[4] a) J. Chmiola, C. Largeot, P.-L. Taberna, P. Simon, Y. Gogotsi, *Science* **2010**, *328*, 480–483; b) G. H. Yu, L. B. Hu, M. Vosgueritchian, H. L. Wang, X. Xie, J. R. McDonough, X. Cui, Y. Cui, Z. N. Bao, *Nano Lett.* **2011**, *11*, 2905–2911; c) Y. W. Zhu, S. Murali, M. D. Stoller, K. J. Ganesh, W. W. Cai, P. J. Ferreira, A. Pirkle, R. M. Wallace, K. A. Cychosz, M. Thommes, D. Su, E. A. Stach, R. S. Ruoff, *Science* **2011**, *332*, 1537–1541.

[5] a) T. Brezesinski, J. Wang, S. H. Tolbert, B. Dunn, *Nat. Mater.* **2010**, *9*, 146–151; b) C. C. Hu, C. Y. Hung, K. H. Chang, Y. L. Yang, *J. Power Sources* **2011**, *196*, 847–850; c) J. W. Liu, J. Essner, J. Li, *Chem. Mater.* **2010**, *22*, 5022–5030; d) S. K. Meher, G. R. Rao, *J. Phys. Chem. C* **2011**, *115*, 15646–15654; e) L. L. Zhang, T. X. Wei, W. J. Wang, X. S. Zhao, *Microporous Mesoporous Mater.* **2009**, *123*, 260–267.

[6] a) J. Gamby, P. L. Taberna, P. Simon, J. F. Fauvarque, M. Chesneau, *J. Power Sources* **2001**, *101*, 109–116; b) C. Vix-Guterl, E. Frackowiak, K. Jurewicz, M. Friebe, J. Parmentier, F. Beguin, *Carbon* **2005**, *43*, 1293–1302.

[7] J. S. Huang, B. G. Sumpter, V. Meunier, *Angew. Chem.* **2008**, *120*, 530–534; *Angew. Chem. Int. Ed.* **2008**, *47*, 520–524.

[8] a) J. Chmiola, C. Largeot, P. L. Taberna, P. Simon, Y. Gogotsi, *Angew. Chem.* **2008**, *120*, 3440–3443; *Angew. Chem. Int. Ed.* **2008**, *47*, 3392–3395; b) J. Chmiola, G. Yushin, Y. Gogotsi, C. Portet, P. Simon, P. L. Taberna, *Science* **2006**, *313*, 1760–1763.

[9] a) H. K. Song, H. Y. Hwang, K. H. Lee, L. H. Dao, *Electrochim. Acta* **2000**, *45*, 2241–2257; b) H. K. Song, Y. H. Jung, K. H. Lee, L. H. Dao, *Electrochim. Acta* **1999**, *44*, 3513–3519.

[10] H. Q. Li, J. Y. Luo, X. F. Zhou, C. Z. Yu, Y. Y. Xia, *J. Electrochem. Soc.* **2007**, *154*, A731–A736.

[11] A. Izadi-Najafabadi, D. N. Futaba, S. Iijima, K. Hata, *J. Am. Chem. Soc.* **2010**, *132*, 18017–18019.

[12] S. Kondrat, C. R. Perez, V. Presser, Y. Gogotsi, A. A. Kornyshev, *Energy Environ. Sci.* **2012**, *5*, 6474–6479.

[13] J. Y. Luo, Y. Y. Xia, *J. Electrochem. Soc.* **2007**, *154*, A987–A992.

[14] a) H. Pang, F. Gao, Q. Chen, R. Liu, Q. Lu, *Dalton Trans.* **2012**, *41*, 5862–5868; b) Q. Wang, Z. Wen, J. Li, *Adv. Funct. Mater.* **2006**, *16*, 2141–2146; c) H. Pang, Q. Y. Lu, C. Y. Chen, X. R. Liu, F. Gao, *J. Mater. Chem.* **2011**, *21*, 13889–13894.

[15] a) O. Lanzi, U. Landau, *J. Electrochem. Soc.* **1991**, *138*, 2527–2538; b) J. W. Weidner, P. Timmerman, *J. Electrochem. Soc.* **1994**, *141*, 346–351.

[16] a) D. N. Futaba, K. Hata, T. Yamada, T. Hiraoka, Y. Hayamizu, Y. Kakudate, O. Tanaike, H. Hatori, M. Yumura, S. Iijima, *Nat. Mater.* **2006**, *5*, 987–994; b) E. Frackowiak, F. Beguin, *Carbon* **2002**, *40*, 1775–1787; c) E. Frackowiak, K. Metenier, V. Bertagna, F. Beguin, *Appl. Phys. Lett.* **2000**, *77*, 2421–2423.

[17] a) See Ref. [4c]; b) C. G. Liu, Z. N. Yu, D. Neff, A. Zhamu, B. Z. Jang, *Nano Lett.* **2010**, *10*, 4863–4868; c) Y. Wang, Z. Q. Shi, Y. Huang, Y. F. Ma, C. Y. Wang, M. M. Chen, Y. S. Chen, *J. Phys. Chem. C* **2009**, *113*, 13103–13107.

[18] X. Y. Lang, A. Hirata, T. Fujita, M. W. Chen, *Nat. Nanotechnol.* **2011**, *6*, 232–236.

[19] R. Liu, S. B. Lee, *J. Am. Chem. Soc.* **2008**, *130*, 2942–2943.

[20] H. L. Wang, H. S. Casalongue, Y. Y. Liang, H. J. Dai, *J. Am. Chem. Soc.* **2010**, *132*, 7472–7477.

[21] Y. Gogotsi, P. Simon, *Science* **2011**, *334*, 917–918.

[22] a) Y. Abe, S. H. Lee, E. O. Zayim, C. E. Tracy, J. R. Pitts, S. K. Deb, *Jpn. J. Appl. Phys. Part 1* **2006**, *45*, 7780–7783; b) A. Devadas, S. Baranton, T. W. Napporn, C. Coutanceau, *J. Power Sources* **2011**, *196*, 4044–4053; c) P. K. Nayak, N. Munichandraiah, *Microporous Mesoporous Mater.* **2011**, *143*, 206–214; d) P. Ragupathy, H. N. Vasan, N. Munichandraiah, *J. Electrochem. Soc.* **2008**, *155*, A34–A40; e) J. P. Zheng, T. R. Jow, *J. Electrochem. Soc.* **1995**, *142*, L6–L8.

[23] a) Q. Lu, M. W. Lattanzi, Y. P. Chen, X. M. Kou, W. F. Li, X. Fan, K. M. Unruh, J. G. G. Chen, J. Q. Xiao, *Angew. Chem.* **2011**, *123*, 6979–6982; *Angew. Chem. Int. Ed.* **2011**, *50*, 6847–6850; b) Q. Lu, Z. J. Mellinger, W. G. Wang, W. F. Li, Y. P. Chen, J. G. G. Chen, J. Q. Xiao, *ChemSusChem* **2010**, *3*, 1367–1370.

